Journal of Environmental Management 411 (2026) 130174

Contents lists available at ScienceDirect

Journal of Environmental Management

journal homepage: www.elsevier.com/locate/jenvman

Research article

Asymmetric recovery of Euro-Mediterranean croplands driven by co-occurring climate forcings

Ramona Magno [a,*,1], Edmondo Di Giuseppe [b,1], Massimiliano Pasqui [b], Leandro Rocchi [a], Sara Quaresima [b], Chi-Farn Chen [c], Chien-Hui Syu [d], Nguyen-Thanh Son [c], Beniamino Gioli [a], Alessandro Matese [a], Salvatore Filippo Di Gennaro [a], Piero Toscano [a,1]

[a] *Institute of BioEconomy, Italian National Research Council, Florence, Italy*
[b] *Institute of BioEconomy, Italian National Research Council, Rome, Italy*
[c] *Center for Space and Remote Sensing Research, National Central University, Taoyuan City, Taiwan*
[d] *Taiwan Agricultural Research Institute, Taichung City, Taiwan*

A R T I C L E I N F O

Keywords:
Asymmetrical crop recovery
Co-occurring extremes
Euro-mediterranean agriculture
Early-warning framework

A B S T R A C T

Euro-Mediterranean croplands are increasingly exposed to co-occurrent climate extremes that threaten productivity. Using satellite-derived Gross Primary Production (2000–2024) across nine major regions, we assessed the resilience of seasonal crop productivity under drought and heat stress. Recovery after winter deficits was rare (3/15 cases, 20%), whereas summer deficits were followed by recovery in the subsequent winter (16/23, 70%). Non-recovery after summer deficits (7/23) consistently coincided with severe prolonged droughts (median affected area ≈80.6%) and positive surface temperature anomalies (median +1.76 °C). By contrast, non-recovery after winter deficits (12/15) was linked either to hot–dry conditions or, less frequently, to cold anomalies with little drought; recovery occurred only when climatic anomalies were weak or absent. These results show that winter conditions set the baseline for annual productivity and constrain summer resilience. Building on this asymmetry, we propose a framework integrating drought-heat indices into early-warning systems and adaptation planning for Euro-Mediterranean agriculture.

1. Introduction

Drought is the second natural disaster affecting global population (CRED, 2026). It can persist from months to years, and intense and long-lasting events are among the costliest hazards (Naumann et al., 2021), causing worldwide multiple impacts and knock-on effects on agricultural productivity, livestock, energy production, waterway transports, and also inducing vegetation dieback (García-León et al., 2021; Jump et al., 2017), especially when it is combined together with other extremes.

Although drought is a recurrent feature of climate, global warming is amplifying its actual and future occurrence, duration, and severity (Büntgen et al., 2021; Hari et al., 2020; Williams et al., 2020), and co-occurrent or cascading hazards are becoming increasingly more frequent and intense (AghaKouchak et al., 2020; Osman et al., 2022; Zscheischler et al., 2018).

Since the beginning of the XXI century, several regions worldwide have experienced prolonged and recurrent droughts, often combined with heat extremes, leading to severe impacts on water availability and agricultural production (ESOTC, 2022) (https://climate.copernicus.eu/esotc/2022/drought) (Medellín-Azuara et al., 2022; Williams et al., 2022; Naumann et al., 2023). Meteorological and climatic extremes can have immediate or delayed negative effects on vegetation, also linked to the phenological stages in which they occur, or indirect effects promoting, for example, the spread of plant pathogens.

From 2000 to 2024 total damages of extreme temperatures and droughts in EU countries amount about 49 billion dollars (EM-DAT, 2025) (https://www.emdat.be/), while climate variability and extreme events have been shown to account for up to 50% of global crop production variability (Frieler et al., 2017; Ray et al., 2015). In Europe,

* Corresponding author.
E-mail addresses: ramona.magno@cnr.it (R. Magno), edmondo.digiuseppe@cnr.it (E. Di Giuseppe), massimiliano.pasqui@cnr.it (M. Pasqui), leandro.rocchi@cnr.it (L. Rocchi), sara.quaresima@cnr.it (S. Quaresima), cfchen@csrsr.ncu.edu.tw (C.-F. Chen), chsyu@tari.gov.tw (C.-H. Syu), ntson@csrsr.ncu.edu.tw (N.-T. Son), beniamino.gioli@cnr.it (B. Gioli), alessandro.matese@cnr.it (A. Matese), salvatorefilippo.digennaro@cnr.it (S.F. Di Gennaro), piero.toscano@cnr.it (P. Toscano).
[1] Ramona Magno, Edmondo Di Giuseppe and Piero Toscano equally contributed to this work.

https://doi.org/10.1016/j.jenvman.2026.130174
Received 27 January 2026; Received in revised form 2 May 2026; Accepted 6 June 2026
Available online 13 June 2026

Brás et al. (2021) estimated an increase of three times of yields decline over the last 50 years due to drought and heat waves, thus also influencing the increase of food commodity prices.

Prolonged rainfall deficit, individually, can already affect crop production (Santini et al., 2022), as well as risk temperatures can impact yields (Lobell et al., 2013), while their co-occurrence can intensify the impacts (Ribeiro et al., 2020).

Nevertheless, a variety of studies on the effects of co-occurrent extremes are limited to specific or few principal crop types e.g., wheat, maize, rice, and soybean at global or national level (Mohammed et al., 2022; Ribeiro et al., 2020; Trnka et al., 2014; Zhao et al., 2022).

The challenge is to understand how and what types of events (their histories) negatively affect vegetation dynamics, the point in time when they can impact croplands, and differences of response across crop types (i.e., spring-summer vs autumn-winter crops) or seasons (Pinke et al., 2022). This knowledge can allow the development of targeted adaptation measures and help farmers to be better prepared for long-term investments (i.e., in more efficient irrigation systems, more resilient crop varieties, cultivation of crops only in the most favourable period of the year, modification of farming practices (Holman et al., 2021) or crops diversification), thus reducing the exposure to economic losses from climatic extremes and at the same time increasing the competitiveness.

These types of information can also support regional and national long-lasting planning by reducing typical ex-post actions, as the compensation, in favour of redirecting and enhancing risk management systems in agriculture (Baldwin and Casalini, 2021) and policies aimed at the sustainability of the sector e.g., the EU's CAP-Common Agricultural Policy and their National Plans.

Moreover, the increasingly frequent co-occurrence of the hot-dry episodes, that can even arise in several regions of the planet in the same period, put at risk not only the farmers' incomes, but also the market stability, the supply chains and the food security in most vulnerable countries (but not only there) (Gaupp et al., 2020), especially for high-water demand crop types. Thus, studying how the co-occurrence of climatic events impacts on yield losses is a prerequisite to assess risks in agriculture sector and to define effective and sustainable mechanisms to improve food systems resilience.

To define climate-yield relationship, studies usually focus on the growing season (Lu et al., 2018), the growth stages (Zhao et al., 2022) or the warmer season, potentially misrepresenting the influence of longer extreme events. Moreover, these approaches typically assess drought–-productivity relationships within a single season or as short-term responses to extreme events, overlooking the potential for carry-over effects across consecutive cropping systems. This represents a critical gap in Euro-Mediterranean agroecosystems, where distinct winter and summer cropping cycles coexist. In this context, the concept of seasonal asymmetry—defined here as the imbalance in recovery potential between consecutive cropping systems (winter → summer vs summer → winter)—provides a novel framework to assess whether productivity deficits in one season can be compensated by the subsequent one.

In this work we examined the Gross Primary Production (GPP) as *proxy* of seasonal ecosystem functioning of the arable crop lands in different Euro-Mediterranean areas together with drought occurrences at different time scales (3, 6 and 12 months) by using the Standardized Precipitation Index (SPI) (McKee et al., 1993), and monthly mean Land Surface Temperature (LST) anomalies during the 2000-2024 period (see Methods), not to analyze their correlation, widely reported into the literature, or create new model for yield forecast (Matiu et al., 2017; Zhang et al., 2025), but to deal with some questions.

1 On the effect of seasonal GPP on the next GPP season to evaluate the agriculture memory of previous GPP reduction.
2 Which, among autumn-winter (Wc) and spring-summer (Sc) crop seasons, are most affected by these dynamics.
3 On the co-occurrent effect of SPI and LST in those dynamics.

And finally providing a policy framework for the future suitability and prediction of Wc and Sc crop seasons in the study area.

2. Materials and methods

2.1. Characterization of the European arable regions under contrasting climates

The study was made in nine arable cropland regions in three European countries: Italy, France, and Hungary (Supplementary Table S1), characterized by different climates ranging from Mediterranean to temperate oceanic and continental (Beck et al., 2018).

Based on estimates of the European Commission (https://agriculture.ec.europa.eu/data-and-analysis/markets/production-data/production-country_en), France, Italy and Hungary are among the first crop producers of the whole EU-27 (Supplementary Fig. S1A–B) in terms of total gross production. Concerning summer crops, France ranked first, while Italy and Hungary ranked third and fourth, respectively (Supplementary Fig. S1B). At subnational level, Emilia Romagna, Piedmont, Sicily, and Tuscany (Grosseto is one of its provinces) are the first, fifth, sixth and tenth main regions in Italy producing cereals, potatoes, vegetables, and legumes (Supplementary Fig. S1C), while Grand Est, Nouvelle Aquitaine, Hauts de France and Centre-Val de la Loire are the first four cereal, oilseed, protein crops and vegetables producers of France (Supplementary Fig. S1D).

2.2. Dataset description

Three main datasets were used in this study: Gross Primary Production (GPP), climate variables (land surface temperature, LST, and precipitation), and land-cover data. Time series of GPP for the period 2001–2024 were constructed for the nine study regions listed in Table S1, using 8-day composite data from the MODIS-Terra global product at 500 m spatial resolution (Running et al., 2015). Corresponding LST time series were derived from hourly ERA5-Land reanalysis data aggregated to monthly means at 0.1° spatial resolution (Muñoz Sabater J., 2019). Precipitation data were obtained from the Multi-Source Weighted-Ensemble Precipitation (MSWEP) dataset, which provides 3-hourly estimates at 0.1° resolution and combines multiple gauge, satellite, and reanalysis precipitation sources, included ERA5 data (Beck et al., 2019). Cropland areas were delineated using the MODIS MCD12C1 land-cover classification (Friedl and Sulla-Menashe, 2022), and all variables were spatially extracted for the cropland classes within each of the nine study sites (Fig. 1).

The inclusion of LST and precipitation was motivated by their direct relevance for the detection of climatic anomalies, whereas GPP was selected as a physiologically based, satellite-derived indicator of vegetation functioning that quantifies carbon uptake through photosynthesis, providing a mechanistic link between climatic drivers and crop productivity (Running et al., 2004) and reflecting the behaviour of highly managed systems. GPP integrates both environmental and physiological constraints, enabling the detection of spatial and temporal variations in productivity and identifying reductions under extreme weather conditions. Its reliability for assessing the impacts of climate variability and extremes on agricultural systems is well established in the literature (Bazzi et al., 2025; Ciais et al., 2005) and confirmed by the comparison with independent regional crop yield statistics (EUROSTAT) (https://ec.europa.eu/eurostat/databrowser/view/apro_cpshr/default/table?lang=en) for both summer and winter crops (Supplementary Fig. S2 A-B).

2.3. Definition of time and space scales aggregation

GPP was aggregated into two seasonal periods representing Euro-Mediterranean functionally relevant cropping systems: the Spring–Summer cropping season (Sc), defined as April to September of the

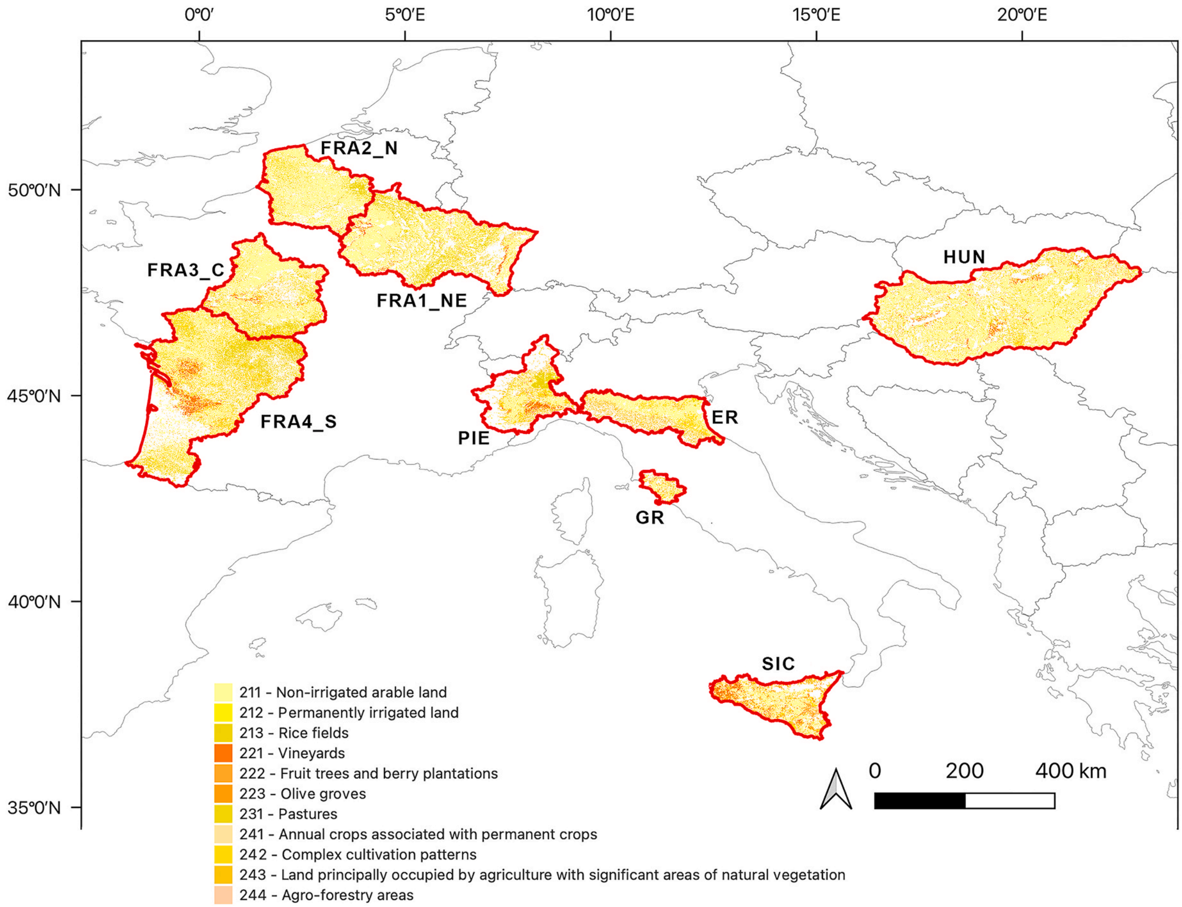

Fig. 1. Geographic extent of the nine study areas across France, Italy, and Hungary and their crop land-cover classes. Map showing the main agricultural land-cover classes considered in the analysis. The red outlines delineate the nine study areas analyzed across France (FRA1_NE, FRA2_N, FRA3_C, FRA4_S), Italy (PIE, ER, GR, SIC), and Hungary (HUN), that cover the entire national territory.

same calendar year, and the Autumn–Winter cropping season (Wc), defined as October of the preceding year through May of the following year, thus including both dormancy and key phases i.e., early growth, vegetative recovery, and, in several regions, the onset of reproductive development. The GPP aggregation windows were defined according to average European crop calendars reported by FAS-USDA database (https://www.fas.usda.gov/data/production/e4). This approach yielded two seasonal GPP time series for each of the nine study regions, comprising 24 seasonal values spanning the period 2000–2024 (2000–2023 for Sc and 2001–2024 for Wc). Due to the marked reduction in GPP observed during Wc 2024 in Sicily, the subsequent Sc 2024 was also included in the analysis. In total, the GPP dataset consists of 216 values (9 regions × 24 observations).

Land Surface Temperature (LST) and precipitation were aggregated at multiple temporal scales to investigate their multi-scale relationships with GPP. While LST can be meaningfully averaged over different periods while preserving spatial comparability, precipitation requires a standardized approach to ensure consistency across time and space. To this end, the original precipitation time series were converted into the Standardized Precipitation Index (SPI), introduced by McKee et al. (1993). The SPI is a probabilistic drought indicator widely adopted for its ability to normalize precipitation anomalies across regions and timescales. SPI was computed at three aggregation periods 3, 6, and 12 months, to capture both short-term (seasonal) and longer-term (multi-seasonal) drought conditions. SPI-1 was not considered because monthly precipitation anomalies may be weakly related to crop water stress due to soil-moisture buffering, whereas SPI-24 and SPI-48 were excluded because they mainly describe multi-year hydrological deficits and smooth the seasonal variability targeted in this study. The index was derived by fitting the aggregated precipitation data to a Gamma distribution and transforming the cumulative probabilities to a standard normal distribution. Consequently, SPI values follow a Gaussian distribution with a mean of zero, where deviations from the mean represent the severity of wet or dry anomalies. Drought severity is classified as moderate ($-1.5 < \mathrm{SPI} \leq -1.0$), severe ($-2.0 < \mathrm{SPI} \leq -1.5$), and extreme ($\mathrm{SPI} \leq -2.0$); wet events are defined analogously on the positive side, while near-normal conditions are $-1.0 < \mathrm{SPI} \leq +1.0$ (McKee et al., 1993). To ensure comparability, LST anomalies were calculated using similar temporal windows (1, 3, 6, and 12 months), allowing the assessment of their co-occurrent and cumulative effects with precipitation on GPP variability.

2.4. Data processing and statistics

To quantify the probability of seasonal recovery after decreased productivity, we first tested the inter-seasonal association between GPP in one crop season and the next using Pearson's correlation test. For each region, we formed two paired series: Sc(t) → Wc(t+1) and Wc(t) → Sc(t), yielding $n = 24$ paired observations per direction. For interpretation, correlations were classified as follows: *moderate* correlation ($r > 0.5$, $p < 0.05$) → seasonal dependency, where productivity in one season is a good predictor of the next; *significant weak* correlation ($0.3 < r < 0.5$, $p < 0.05$) → statistically significant but moderate relationship, indicating a real seasonal link though weaker in strength; *weak* correlation ($0.3 < r < 0.5$, $p > 0.05$) → some seasonal influence, where a relationship exists but climate variability likely plays a bigger role in seasonal recovery; and *no correlation* ($r < 0.3$, $p > 0.05$) → independent seasonal behaviour, where productivity in one season does not strongly predict the next, implying recovery is largely independent from prior seasonal conditions. The results are presented in Supplementary Table S2, where *moderate* and *weak* correlations are indicated based on the Pearson correlation values. The table also provides the corresponding p-values to highlight statistical significance. For both seasonal aggregations (Sc and Wc), we identified periods marked by reductions in primary production. Prior to standardization, we tested the normality of GPP distributions within each region using the Shapiro–Wilk test. Since the results indicated that GPP values followed an approximately Gaussian distribution, we proceeded to standardize the data by transforming the empirical values into z-scores with a mean of zero and a standard deviation of one. Each standardized GPP anomaly was calculated relative to the regional mean, dividing the deviation by the corresponding standard deviation. This normalization minimizes regional differences in GPP magnitude while ensuring comparability across study areas. We then applied a threshold to the cumulative distribution of standardized GPP values across all regions to identify the strongest declines in GPP during 2000–2024. Years exhibiting markedly negative anomalies were defined using a threshold of $z = -1.3$, corresponding to approximately the lowest 10% of observations in a near-Gaussian distribution. This threshold represents a balance between statistical robustness and operational sensitivity and is consistent with similar applications in environmental monitoring, where moderate standardized anomalies have been shown to capture meaningful climatic and vegetational changes (Verdugo et al., 2024). Recovery was defined as the return of standardized GPP anomalies to values equal to or above the long-term mean ($z \geq 0$) in the season following a negative anomaly ($z \leq -1.3$). *Asymmetric recovery* was defined as the imbalance in recovery frequency between the two seasonal transitions. LST anomalies were computed to align the three variables, LST-GPP-SPI, under a standardized deviation framework centred on zero. We also identified the most pronounced LST anomalies (thresholds of ± 1 °C) across four temporal scales (1, 3, 6, and 12 months) and quantified the percentage of area affected by severe-to-extreme drought, defined as SPI ≤ -1.5.

All variables were aggregated at the regional level to emphasize large-scale, coherent signals in agroecosystem functioning, consistent with the study objective of identifying seasonal patterns rather than field-scale variability. While spatial aggregation may smooth localized extremes, this effect was mitigated by using the percentage of area affected by severe–extreme drought classes of SPI, rather than spatial averages, thereby preserving the signal of spatially heterogeneous stress conditions.

This integrated framework allowed us to analyze the co-occurrence of climatic forcings associated with the most negative GPP anomalies, comparing multi-temporal LST (1–12 months) and SPI (3–12 months) signals.

All the analysis was performed in R (Team, 2016) (https://www.R-project.org/) and Matlab (The MathWorks Inc, 2022) (https://www.mathworks.com).

3. Results

3.1. Seasonal GPP memory analysis

Pearson correlation analysis between seasonal GPP values (Supplementary Table S2) revealed contrasting patterns depending on the direction of the pairing. When Spring–Summer (Sc) GPP was related to the following Autumn–Winter season (Wc) (Sc→Wc) two groups were identified, and no statistically significant correlations emerged.

- *weak (non-significant) negative correlation* ($-0.342 \leq r \leq -0.383$ and $0.064 \leq p \leq 0.102$) i.e., FRA3_C, FRA1_NE, HUN;
- *no correlation* ($-0.231 \leq r \leq -0.020$) i.e., ER, PIE, GR, SIC, FRA4_S, FRA2_N.

Conversely, when Autumn–Winter (Wc) GPP was compared with the subsequent Spring–Summer (Sc) season (Wc→Sc), areas were grouped in three, and some clearer signals of an inter-seasonal "memory" emerged.

- *moderate significant positive correlation* ($0.513 \leq r \leq 0.525$ and $0.0101 \leq p \leq 0.0122$) i.e., FRA3_C, FRA2_N;
- *significant weak positive correlation* ($0.415 \leq r \leq 0.476$ and $0.0217 \leq p \leq 0.0489$) i.e., SIC, FRA1_NE, HUN, indicating that winter productivity meaningfully influences the subsequent summer, albeit with more moderate strength;
- *no correlation* ($0.100 \leq r \leq 0.278$ and $0.199 \leq p \leq 0.650$) i.e., ER, PIE, GR, FRA4_S, fell into the no-correlation category, consistently showed no inter-seasonal coupling in either direction.

3.2. Extreme anomalies and seasonal recovery

Given the directional asymmetry detected in the correlation analysis with Autumn-Winter crop season (Wc) GPP exerting some influence on the subsequent Spring–Summer crop season (Sc) GPP than vice versa, we further investigated recovery capacity following extreme seasonal productivity deficits. To find the strongest GPP anomalies, thresholds were derived from the cumulative distribution functions of standardized GPP (Fig. 2), corresponding to -1.3 units of standard deviation (STD), which captures approximately the lowest 7% of Wc GPP and 11% of Sc GPP values.

Table 1 lists all years in which each study area experienced a negative seasonal anomaly beyond the -1.3 STD threshold. For each case, we evaluated whether the subsequent season recovered to at least the long-term mean GPP.

Recovery rates were notably asymmetric between the two seasonal sequences (Table 1). Following Sc anomalies, 16 out of 23 cases (around 70%) were followed by a Wc season with GPP values equal to or exceeding the long-term mean. In contrast, after Wc anomalies, only 3 out of 15 cases (20%) saw recovery in the subsequent Sc season. This highlights a greater resilience of Wc crop season to preceding summer deficits, whereas summer recovery from severe winter losses is rare.

In ER, the Sc anomaly of 2003 was followed by a further anomaly in 2004 (Wc), and similarly the 2012 Sc anomaly was followed by a negative Wc in 2013, indicating repeated non-recovery events.

In PIE, the Sc anomaly of 2003 was not followed by recovery, while the 2006 anomaly was followed by a strong recovery in Wc (2007). More recently, the 2022 Sc anomaly was not compensated, with the subsequent Wc slightly below average; notably, it followed a Wc anomaly in the same year.

In GR, recovery occurred after the 2003 Sc anomaly (Wc, 2004), but not after the 2018 Sc anomaly, which was followed by a negative Wc (≈ -1.2 STD). Similarly, Wc anomalies in 2003 and 2009 were not followed by recovery.

In SIC, all Sc anomalies were followed by recovery, whereas none of the Wc anomalies were compensated. Instead, subsequent Sc seasons often showed further anomalies, including 2002 and 2024, the latter reaching -2.1 STD, the lowest value in the series.

In FRA4_S, all Sc anomalies were followed by recovery, while both Wc anomalies were not compensated in the subsequent Sc seasons.

In FRA3_C, recovery occurred only after the 2006 Sc anomaly, whereas anomalies in 2013 (Wc) and 2016 (Sc) were followed by further negative conditions.

In FRA2_N, both Sc anomalies were followed by recovery, while the 2013 Wc anomaly was not, being embedded between two negative Sc seasons.

In FRA1_NE, all Sc anomalies were followed by recovery, whereas Wc anomalies in 2013 and 2021 were not compensated.

In HUN, Sc anomalies in 2003 and 2022 were followed by recovery, while the 2012 event was not; notably, the 2022 Sc anomaly followed a strong Wc anomaly. Conversely, Wc anomalies in 2003 and 2021 were

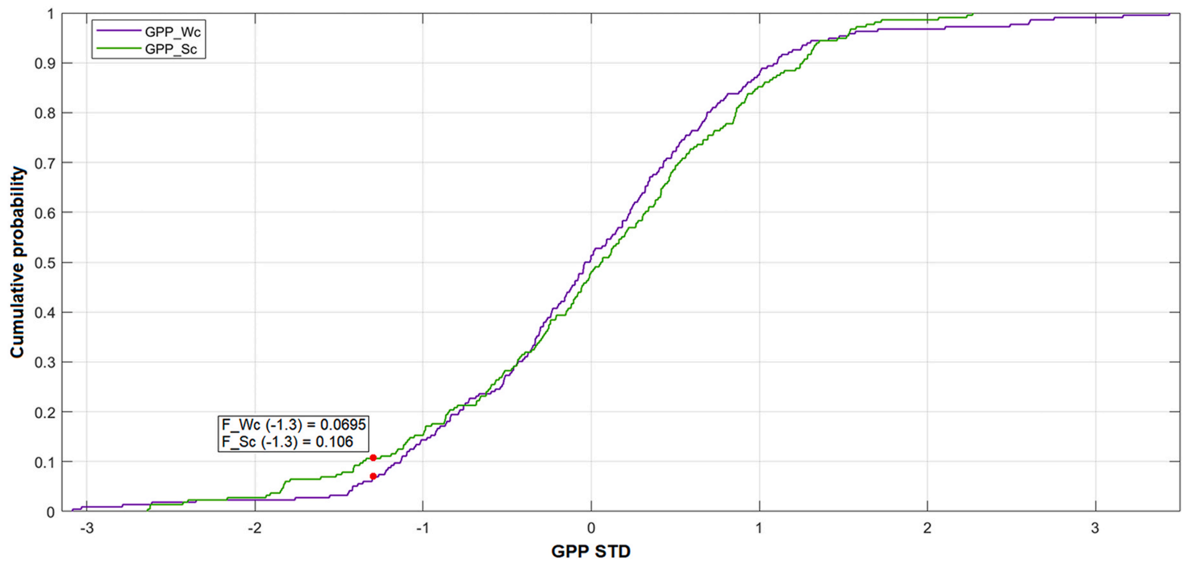

Fig. 2. Cumulative probability distributions of standardized GPP for autumn–winter (Wc) and spring–summer (Sc) seasons. Cumulative distribution functions (CDFs) of standardized gross primary productivity (GPP) for Wc (purple) and Sc (green) across all study regions. The thresholds corresponding to −1.3 standard deviations (STD) are indicated, marking the lower-tail conditions associated with reduced productivity.

Table 1
Years with strongest negative GPP anomalies across study areas and crop seasons. Years with strongest gross primary productivity (GPP) anomalies (below −1.3 STD) identified for each area and crop season. In bold are highlighted, for each area, two consecutive (Sc→Wc or Wc→Sc) seasons with strongest GPP anomalies. Asterisks denote years in which recovery occurred during the subsequent crop season. Only for Sicily, Sc 2024 was also included, as it was affected by strong anomalies and coupled with the preceding negative anomaly in Wc (2024).

Areas	Sc Anomalies	Wc Anomalies
ER	**2003**, 2012	**2004***
PIE	2003, 2006*, 2022	2009*, 2018*
GR	**2003***, 2017	**2003**, 2009
SIC	**2002***, 2016*, 2022*, **2024**	**2002**, 2024
FRA4_S	2003*, 2006*, 2022*	2009, 2013
FRA3_C	2006*, 2016	2013
FRA2_N	2001*, 2006*	2013
FRA1_NE	2001*, 2003*, 2006*	2013, 2021
HUN	**2003***, 2012, 2022*	**2003**, 2021

not followed by recovery.

3.3. Co-occurring climate forcings behind strong GPP anomalies

The combined analysis of GPP anomalies with severe-extreme drought extent (SPI) and Land Surface Temperature (LST) anomalies revealed distinct patterns of co-occurrence that shaped the capacity of croplands to recover in the subsequent season.

Among the 15 strong Wc anomalies (≤−1.3 STD) (Fig. 3A), the large majority (12 cases) were not recovered in the following Sc (Fig. 3B). These cases clustered into two main patterns: (i) positive LST anomalies combined with widespread severe-extreme drought, or (ii) colder-than-average anomalies, most often concentrated in LST1 (May), with only minimal or no-drought extent (median ≈ 2.5% of territory). A notable outlier was FRA4_S in 2009, where the negative anomaly was long-term (LST12), coupled with a SPI6 signal leading to ≈ 37% of the study area being affected by severe-extreme drought. These conditions suggest that when drought starts in winter, even if relatively limited, it is often associated with reduced recovery in the subsequent Sc. GR 2009 was another special case, not falling within the main clusters: no SPI signal was detected, the major forcing being a positive LST1 anomaly (+1.66 °C), and the year was also marked by a collapse in fall/winter cereal sowing (ISTAT) (https://esploradati.istat.it/databrowser/) (≈50% reduction). Even if the GPP time series are detrended, such agronomic disruptions may still contribute to the strongest anomalies not fully explained by climatic co-occurrences.

By contrast, only three Wc anomalies were followed by recovery in the subsequent Sc. In these cases, climate anomalies were generally weak or absent. The main exception was ER 2004, which showed a strong cold anomaly (LST1 = −1.9 °C) and severe-extreme drought affecting ≈ 13% of the territory. Another distinctive case was 2018 in PIE, where no SPI or LST anomalies were evident. However, this GPP anomaly followed a very low Sc in 2017 (−1 STD) and coincided with an extreme late-winter cold event, especially in minimum temperatures, and above average rainfall in spring and during the ripening phase (Agricoltura.it, 2018; ARPA Piemonte, 2018) (https://www.agricultura.it/2018/11/13/focus-piemonte-2018-landamento-delle-produzioni-agricole/; https://www.arpa.piemonte.it/pubblicazione/clima-piemonte-anno-2018).

Strong Sc anomalies occurred 23 times (Fig. 4A), of which 7 were not recovered in the following Wc season (Fig. 4B). These non-recovery events were consistently associated with severe climatic stress: long-term (SPI12) and very large severe-extreme drought extent (median ≈ 80.6% of territory), and strongly positive LST anomalies (median +1.76 °C), except for 2017 at −1.23 °C. The most frequent LST anomaly window was LST6 (April-September), underlining the role of prolonged summer heat in driving productivity collapses that were not compensated in the subsequent Wc season.

Furthermore, for Sc season the signal of co-occurrence of prolonged and intense hot-dry events influencing non-recovered negative GPP anomalies (Fig. 4B) is stronger and more coherent compared to the Wc season (Fig. 3B).

In contrast, most of Sc anomalies (16 cases) were followed by recovery in the subsequent Wc season. Here, severe-extreme drought extent was much smaller (median ≈ 11.1%, mostly below 30%), with the sole exception of 2002 in Sicily (>80%). This anomaly was rapidly compensated in winter 2003 thanks to abundant rainfall and cooler temperatures (SIAS, 2003) (http://www.sias.regione.sicilia.it/analisi_2003/WEB/Meteoclima_2003.pdf).

LST anomalies in recovery cases varied in sign but were most often concentrated in the latest monthly window (LST1). SPI12 remained the most recurrent drought signal, although its magnitude was weaker

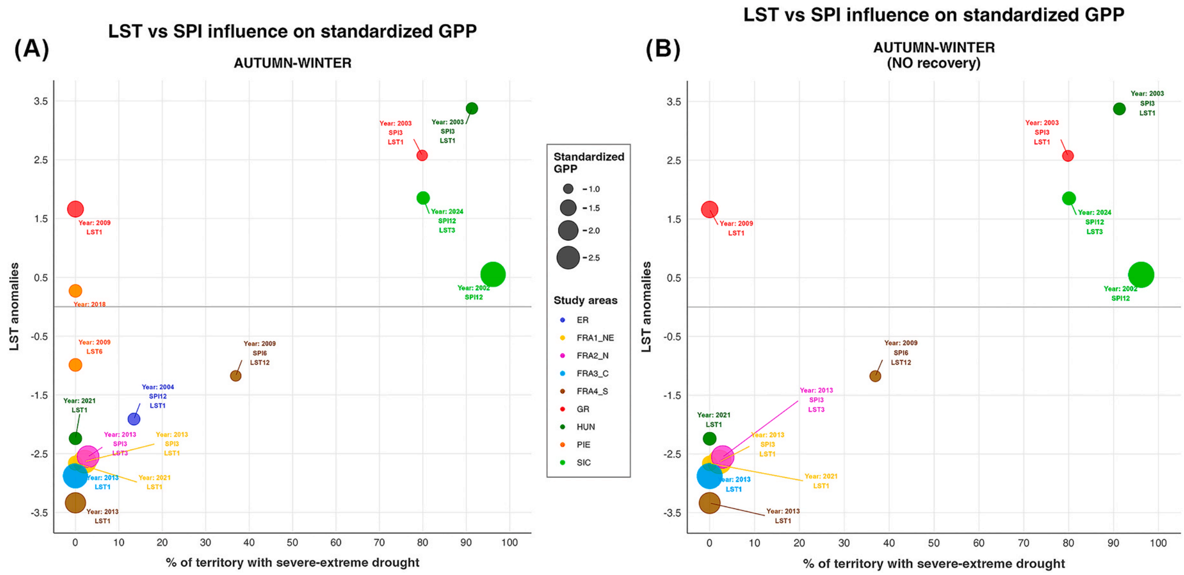

Fig. 3. Climatic drivers of negative GPP anomalies during the autumn–winter (Wc) crop season across European arable regions. (A) Relationship between the percentage of territory affected by severe-to-extreme drought (SPI) and land surface temperature (LST) anomalies for all Wc GPP anomalies below −1.3 standard deviations (STD). (B) Same as in (A) but limited to Wc GPP anomalies not followed by recovery in the subsequent spring–summer (Sc) season. Bubble size is proportional to the magnitude of the standardized GPP anomaly. Labels indicate the year, and the dominant climatic variables associated with each anomaly, while different colours represent the nine study areas.

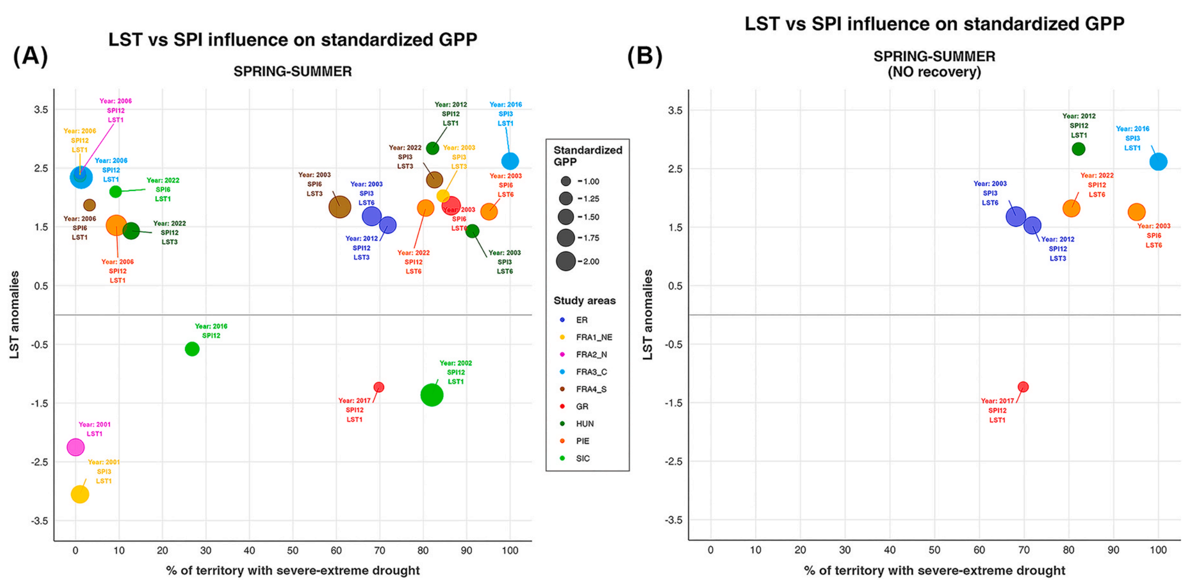

Fig. 4. Climatic drivers of negative GPP anomalies during the spring–summer (Sc) crop season across European arable regions. (A) Relationship between the percentage of territory affected by severe-to-extreme drought (SPI) and land surface temperature (LST) anomalies for all Sc GPP anomalies below −1.3 standard deviations (STD). (B) Same as in (A) but limited to Sc GPP anomalies not followed by recovery in the subsequent autumn–winter (Wc) season. Bubble size is proportional to the magnitude of the standardized GPP anomaly. Labels indicate the year, and the dominant climatic variables associated with each anomaly, while different colours represent the nine study areas.

compared to non-recovered events.

3.4. Policy framework for anticipating crop season recovery

Building on the co-occurrence analysis of LST and SPI, we derive a forecast-oriented framework (Fig. 5) from the observed patterns to anticipate the likelihood of recovery following strong seasonal GPP anomalies. The approach does not rely on real-time GPP estimates, which are not available early in the season, but instead uses operationally accessible climate indicators and seasonal forecasts. Two main rules emerge from the observed asymmetry in seasonal resilience. First, when anomalies occur in Autumn–Winter (Wc), recovery in the subsequent Spring–Summer (Sc) is rare. In these cases, forecasted warm anomalies (LST1 or LST3 $>$ +1.5 °C) combined with severe-extreme negative SPI3/SPI12 or drought extent >30% consistently correspond to high-risk configurations identified in the observed dataset and can therefore be interpreted as high-alert conditions, characterized by a strong likelihood of continued GPP depression. Conversely, when Wc anomalies co-occur with neutral SPI and limited drought extent (<20%) under cool or neutral LST signals, partial recovery is still possible, as observed in a few exceptional cases.

Second, when anomalies occur in Spring–Summer (Sc), recovery in

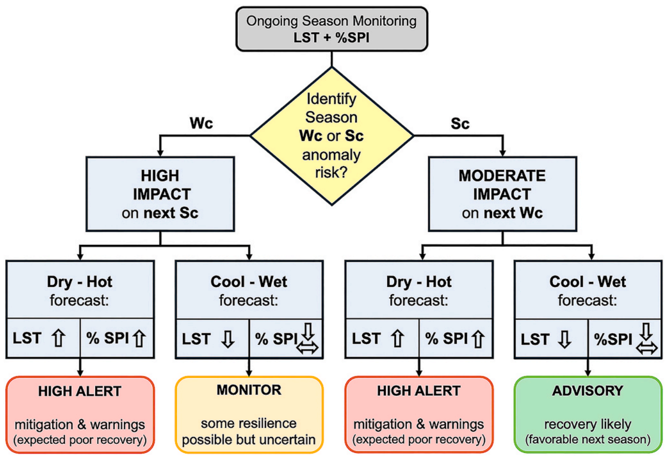

Fig. 5. Forecast-oriented policy framework for anticipating seasonal recovery in GPP based on co-occurrent climatic anomalies. Flowchart summarizing the proposed decision framework derived from the co-occurrence analysis of land surface temperature (LST) and drought extent (%SPI). The scheme identifies the active anomaly season—autumn–winter (Wc) or spring–summer (Sc)—and classifies the expected impact on the subsequent crop season according to forecasted LST and SPI conditions.

the following Wc is more frequent, but it remains contingent on the absence of extensive drought signals. Negative and widespread SPI3/SPI12 combined with positive LST1/LST6 anomalies (>+1.5 °C) were consistently associated with persistence of low productivity, whereas recovery was more commonly observed when SPI trends stabilized and LST anomalies were weak or negative.

This framework translates observed co-occurrence patterns into an operational decision scheme, linking anomaly classification and forecasted conditions to recovery likelihood and associated risk levels for the subsequent season.

4. Discussion

The analysis of seasonal GPP anomalies across Euro-Mediterranean croplands reveals a distinct asymmetry in inter-seasonal dynamics. While strong Spring–Summer (Sc) anomalies were frequently followed by recovery in the subsequent Autumn–Winter (Wc), the reverse pattern was rarely observed: deficits emerging in Wc often persisted, constraining productivity in the following Sc. This unidirectional dependency suggests that winter conditions play a decisive role in shaping the annual trajectory of crop productivity. The winter period considered here does not represent a purely dormant phase, but integrates crop establishment, vegetative development, and recovery processes, allowing GPP to capture overall system functioning across distinct cropping cycles. In this context, winter deficits reflect negative anomalies relative to the expected seasonal trajectory, rather than reductions from a biologically inactive baseline. The finding is particularly evident in central and northern France, Hungary and Sicily, where Moderate to Significant Weak Wc→Sc *correlations* indicate that anomalies in the cooler season can carry over into summer, amplifying risks of productivity loss. Other regions showed little inter-seasonal dependency, pointing to a greater resilience to short-term variability. These spatially differentiated patterns align with earlier findings that highlight the Euro-Mediterranean basin as a climate change hotspot, where the co-occurrence of temperature and drought extremes increasingly governs crop performance (Bento et al., 2021; He et al., 2022). As further confirmation, Giaquinto et al. (2025) highlighted an increase in hot/dry compound events also in central-eastern European regions, both in winter and especially in summer. The strong influence of Wc conditions on Sc outcomes observed here is consistent with the broader understanding of Euro-Mediterranean cropping systems. Surface and ground water accumulation during autumn and winter is critical for determining the water availability for summer crops, indicating that unfavourable Wc anomalies are associated with a reduced baseline capacity of ecosystems to sustain growth later in the year.

In contrast, severe summer anomalies, though often widespread and destructive, may be partially compensated when the following winter is cool and wet. This finding resonates with recent work showing that increases in January–March temperatures can enhance wheat yields in northern and eastern Europe, partly offsetting the negative impact of summer warming (Pinke et al., 2022). These results reinforce the idea that agricultural vulnerability in Euro-Mediterranean systems is unevenly distributed across seasons, being strongly conditioned by winter dynamics. They also provide further evidence on the role of co-occurring climate extremes. Previous studies have shown that the combination of drought and heat amplifies crop losses compared to individual hazards (Ribeiro et al., 2020), with drought acting as the dominant stressor in Mediterranean systems. This is consistent with the carry-over mechanisms identified here, where winter deficits can establish baseline vulnerabilities that co-occur with subsequent hot/dry summers, amplifying productivity losses. In line with He et al. (2022), these findings highlight the importance of considering multivariate interactions, as even moderate Wc anomalies may lead to disproportionate impacts when combined with summer stressors. While management practices can modulate these responses, the GPP signal captures the integrated behavior of agroecosystems, retaining a robust climatic imprint supported by independent LST and SPI indicators.

From this perspective, it is crucial to complement near real-time monitoring with seasonal forecasts at 3-6 months lead times, providing insight into the meteo-climatic conditions that may exacerbate an already critical situation in the following season. The approach proposed by Brands et al. (2025) aligns with this need, advocating for the integration of SPEI-based forecasts into operational climate service frameworks. Proctor et al. (2025) also emphasize the importance of jointly analyzing thermal and water-related factors on increasing yield volatility, but from a broader perspective of climate projections. In doing so, they close the knowledge loop, which — starting from operational support for crop management through effective monitoring and forecasting — leads to the planning of long-term adaptation measures.

A comparison between GPP-based recovery signals and subsequent yield outcomes (data not shown) revealed a high level of consistency, with only 6 mismatches out of 38 cases, including 3 winter crop cases in France around 2007, likely associated with excess precipitation during reproductive stages affecting yield more than biomass (Aubry et al., 2026).

A further consideration concerns the use of statistical thresholds for identifying strong anomalies. The −1.3 STD cutoff adopted in this study provided a consistent benchmark, yet the experience of 2022 illustrates the limitations of a rigid thresholding approach. In that year, Wc GPP in Emilia-Romagna, Piedmont, Tuscany, and Sicily was markedly below average, though it remained just above −1.3 STD. Moreover, despite seasonal forecasts had already signalled a hot/dry Sc, agricultural policy favoured the expansion of summer crops such as maize. The result was a collapse of Sc GPP, which crossed the −1.3 STD threshold in Sicily and Piedmont. Indeed, 2022 was characterized by extreme drought, which was reflected in the agriculture production (Tripathy and Mishra, 2023). This outcome does not undermine the framework proposed here; rather, it highlights that near-threshold years can follow the same dynamics as formally defined anomalies and should be treated as high-risk cases within monitoring systems. This assumption is also confirmed by a retrospective analysis of GPP negative values near −1.3 STD threshold and corresponding to prolonged LST and SPI extremes during the Wc period that preceded an Sc with a strong negative anomaly (with STD < −1.3).

Moreover, additional sensitivity checks including near-zero GPP negative anomalies showed that relaxing the recovery threshold does not alter—and, in the case of summer deficits followed by winter recovery, even strengthens (from 70% to 82%)—the observed asymmetry. Although these cases reflect substantial improvements without fully reaching the long-term mean, the overall dynamics remain unchanged, supporting the use of $z \geq 0$ as a consistent and interpretable recovery criterion.

Current early warning systems are potentially effective, but, being largely based on climatic assessments, they are often overlooked. A relevant example is the EU decision, taken in response to the Russia–Ukraine war, to allow—on an exceptional and temporary basis—the cultivation of spring–summer crops on fallow land, despite a dry winter and seasonal forecasts indicating extreme drought conditions for the subsequent six months. There is a lack of contextualization with respect to the signals of memory and asymmetry in both the phenomena and the response of vegetation.

From a policy perspective, these results carry three key implications. First, early-warning systems must explicitly account for the asymmetry of seasonal dependencies to be more effective. In practice, this means that Wc anomalies should be treated as strong predictors of systemic risk in the subsequent Sc, while Sc anomalies require careful monitoring but allow for greater recovery potential. Second, adaptive strategies should be particularly cautious in promoting crop expansion or water-intensive species cultivation after Wc anomalies, especially when seasonal forecasts indicate warm/dry conditions for the upcoming summer. Third, a rigid definition of the statistical anomaly threshold may fail to identify situations that trigger crises (as in 2022). Instead, it should be combined with a probabilistic classification for both monitoring and forecasting. This would ensure more effective operational climate services to support proactive adaptation measures.

By doing so, adaptation policies can be better aligned with early-warning signals, prioritizing water conservation, sowing adjustments, and crop choice when recovery is unlikely, and capitalizing on favourable forecasts when resilience is expected.

The proposed framework represents a step forward in this direction by integrating monitoring and forecasting systems with vegetation response analysis, moving toward a more comprehensive and informative support system.

5. Conclusions

Our analysis highlights a pronounced asymmetry in the recovery capacity of Euro-Mediterranean croplands under co-occurrent climate extremes. Winter productivity deficits rarely recovered in the subsequent summer, whereas summer anomalies were more often compensated in the following winter, provided that drought and heat stress were limited. These results underscore the strong association between winter conditions and annual agricultural trajectories and demonstrate the value of integrating compound indicators—such as SPI and LST—into operational monitoring. The proposed framework can be further strengthened by advances in Earth observation and climate services, including high-resolution GPP products, solar-induced fluorescence (SIF) observations, forthcoming missions such as Copernicus FLEX, and improved seasonal forecasts. By linking forecasted drought and temperature conditions to recovery likelihood, this approach supports more informed decisions on sowing strategies, irrigation management, and crop selection. Ultimately, it provides a basis for early-warning systems that move from reactive responses toward proactive adaptation under increasingly frequent hot–dry extremes.

CRediT authorship contribution statement

Ramona Magno: Conceptualization, Data curation, Formal analysis, Methodology, Validation, Visualization, Writing – original draft, Writing – review & editing. **Edmondo Di Giuseppe:** Conceptualization, Data curation, Formal analysis, Methodology, Validation, Visualization, Writing – original draft, Writing – review & editing. **Massimiliano Pasqui:** Validation, Visualization. **Leandro Rocchi:** Data curation, Formal analysis. **Sara Quaresima:** Data curation, Visualization. **Chi-Farn Chen:** Validation. **Chien-Hui Syu:** Resources, Validation. **Nguyen-Thanh Son:** Validation. **Beniamino Gioli:** Validation. **Alessandro Matese:** Validation. **Salvatore Filippo Di Gennaro:** Validation. **Piero Toscano:** Conceptualization, Data curation, Formal analysis, Methodology, Resources, Supervision, Validation, Visualization, Writing – original draft, Writing – review & editing.

Declaration of competing interest

The authors declare that they have no known competing financial interests or personal relationships that could have appeared to influence the work reported in this paper.

Acknowledgements

This research paper was produced within the activities of the Geospatial big data analytics for climate-smart agricultural practices project, Bilateral Agreement National Research Council – Italy/National Science Technology Council – Taiwan, Joint Research Projects N. 0091275/2022 and N. 112-2927-I-055-502.

Appendix A. Supplementary data

Supplementary data to this article can be found online at https://doi.org/10.1016/j.jenvman.2026.130174.

Data availability

The datasets generated and/or analyzed during the current study are available at the following URL's: - MODIS-Terra global datasets of GPP and are available at [https://lpdaac.usgs.gov/product_search/]; - ERA5-Land hourly data of LST are available at [https://cds.climate.copernicus.eu/datasets]; - Global precipitation data from *MSWEP - Multi-Source Weighted-Ensemble Precipitation* dataset are available at [https://www.gloh2o.org/mswep/]; - MODIS MCD12C1 Land cover type data are available at [https://lpdaac.usgs.gov/products/mcd12c1v061/].

References

AghaKouchak, A., Chiang, F., Huning, L.S., Love, C.A., Mallakpour, I., Mazdiyasni, O., Moftakhari, H., Papalexiou, S.M., Ragno, E., Sadegh, M., 2020. Climate extremes and compound hazards in a warming world. Annu. Rev. Earth Planet Sci. 48, 519–548. https://doi.org/10.1146/annurev-earth-071719-055228.

Agricoltura.it – Il giornale dell'agricoltura italiana, 2018. Focus Piemonte. L'andamento delle produzioni Agricole.

ARPA Piemonte, 2018. Il Clima in Piemonte - Anno 2018.

Aubry, M., Renard, B., Opitz, T., Le Roux, R., Launay, M., García de Cortázar-Atauri, I., Furusho-Percot, C., 2026. From past exceptional extremes to frequent future risks: how climate change shapes the fate of common wheat in France. Agric. For. Meteorol. 379, 111054. https://doi.org/10.1016/j.agrformet.2026.111054.

Baldwin, K., Casalini, F., 2021. Building the Resilience of Italy's Agricultural Sector to Drought. Paris.

Bazzi, H., Ciais, P., Makowski, D., Baghdadi, N., 2025. Advancing winter wheat yield anomaly prediction with high-resolution satellite-based gross primary production. One Earth 8.

Beck, H.E., Wood, E.F., Pan, M., Fisher, C.K., Miralles, D.G., van Dijk, A.I.J.M., McVicar, T.R., Adler, R.F., 2019. MSWEP V2 global 3-Hourly 0.1° precipitation: methodology and quantitative assessment. Bull. Am. Meteorol. Soc. 100, 473–500. https://doi.org/10.1175/BAMS-D-17-0138.1.

Beck, H.E., Zimmermann, N.E., McVicar, T.R., Vergopolan, N., Berg, A., Wood, E.F., 2018. Present and future Köppen-Geiger climate classification maps at 1-km resolution. Sci. Data 5, 180214. https://doi.org/10.1038/sdata.2018.214.

Bento, V.A., Ribeiro, A.F.S., Russo, A., Gouveia, C.M., Cardoso, R.M., Soares, P.M.M., 2021. The impact of climate change in wheat and barley yields in the iberian Peninsula. Sci. Rep. 11, 15484.

Büntgen, U., Urban, O., Krusic, P.J., Rybníček, M., Kolář, T., Kyncl, T., Ač, A., Koňasová, E., Čáslavský, J., Esper, J., Wagner, S., Saurer, M., Tegel, W., Dobrovolný, P., Cherubini, P., Reinig, F., Trnka, M., 2021. Recent European drought extremes beyond common Era background variability. Nat. Geosci. 14, 190–196. https://doi.org/10.1038/s41561-021-00698-0.

Brands, S., Iturbide, M., Díez González-Pardo, J., Herrera, S., Bedia, J., Manzanas, R., Rodríguez-Guisado, E., Beguería, S., Vicente-Serrano, S.M., Gutiérrez, J.M., 2025. Seasonal drought predictions in the mediterranean using the SPEI index: paving the way for their operational applicability in climate services. Clim. Serv. 38, 100555. https://doi.org/10.1016/j.cliser.2025.100555.
Brás, T.A., Seixas, J., Carvalhais, N., Jägermeyr, J., 2021. Severity of drought and heatwave crop losses tripled over the last five decades in Europe. Environ. Res. Lett. 16, 065012. https://doi.org/10.1088/1748-9326/abf004.
Ciais, P., Reichstein, M., Viovy, N., Granier, A., Ogée, J., Allard, V., Aubinet, M., Buchmann, N., Bernhofer, C., Carrara, A., 2005. Europe-wide reduction in primary productivity caused by the heat and drought in 2003. Nature 437, 529–533.
Delforge, D., Below, R., Wathelet, V., Tonnelier, M., Alonso, A., Speybroeck, N., 2026. 2025 Disasters in Numbers. Centre for Research on the Epidemiology of Disasters (CRED), Brussels, Belgium.
EM-DAT, Centre for Research on the Epidemiology of Disasters (CRED). (last access: 22 August 2025).
European State of the Climate, 2022. ESOTC last access July 2025.
European Commission - Agriculture and Rural Development. Production by Country.(last access: July 2025).
EUROSTAT. Crop production in EU standard humidity by NUTS 2 region. https://doi.org/10.2908/APRO_CPSHR. (last access April 15, 2026).
Foreign Agricultural Service, 2025. U.S. Department of Agriculture (FAS-USDA) last access July 2025.
Friedl, M., Sulla-Menashe, D., 2022. MODIS/Terra+ Aqua Land Cover Type Yearly L3 Global 0.05 Deg CMG V061. NASA EOSDIS Land Processes Distributed Active Archive Center (DAAC) Data Set MCD12C1-061.
Frieler, K., Schauberger, B., Arneth, A., Balkovič, J., Chryssanthacopoulos, J., Deryng, D., Elliott, J., Folberth, C., Khabarov, N., Müller, C., Olin, S., Pugh, T.A.M., Schaphoff, S., Schewe, J., Schmid, E., Warszawski, L., Levermann, A., 2017. Understanding the weather signal in national crop-yield variability. Earths Future 5, 605–616. https://doi.org/10.1002/2016EF000525.
García-León, D., Standardi, G., Staccione, A., 2021. An integrated approach for the estimation of agricultural drought costs. Land Use Policy 100, 104923. https://doi.org/10.1016/j.landusepol.2020.104923.
Gaupp, F., Hall, J., Hochrainer-Stigler, S., Dadson, S., 2020. Changing risks of simultaneous global breadbasket failure. Nat. Clim. Change 10, 54–57.
Giaquinto, D., Di Capua, G., Marzocchi, W., Kurths, J., 2025. Spatio-temporal evolution of compound hot and dry extremes synchronizations in Europe. Clim. Dyn. 63, 1–21.
Hari, V., Rakovec, O., Markonis, Y., Hanel, M., Kumar, R., 2020. Increased future occurrences of the exceptional 2018–2019 Central European drought under global warming. Sci. Rep. 10, 12207. https://doi.org/10.1038/s41598-020-68872-9.
He, Y., Hu, X., Xu, W., Fang, J., Shi, P., 2022. Increased probability and severity of compound dry and hot growing seasons over world's major croplands. Sci. Total Environ. 824, 153885. https://doi.org/10.1016/j.scitotenv.2022.153885.
Holman, I., Hess, T., Rey, D., Knox, J., 2021. A multi-level framework for adaptation to drought within temperate agriculture. Front. Environ. Sci. 8. https://doi.org/10.3389/fenvs.2020.589871.
ISTATData - The Italian National Institute of Statistics data warehouse. Istat Data Browser v4.1.12.(last access: July 2025).
Jump, A.S., Ruiz-Benito, P., Greenwood, S., Allen, C.D., Kitzberger, T., Fensham, R., Martínez-Vilalta, J., Lloret, F., 2017. Structural overshoot of tree growth with climate variability and the global spectrum of drought-induced forest dieback. Glob. Change Biol. 23, 3742–3757. https://doi.org/10.1111/gcb.13636.
Lobell, D.B., Hammer, G.L., McLean, G., Messina, C., Roberts, M.J., Schlenker, W., 2013. The critical role of extreme heat for maize production in the United States. Nat. Clim. Change 3, 497–501.
Lu, Y., Hu, H., Li, C., Tian, F., 2018. Increasing compound events of extreme hot and dry days during growing seasons of wheat and maize in China. Sci. Rep. 8, 16700. https://doi.org/10.1038/s41598-018-34215-y.
Matiu, M., Ankerst, D.P., Menzel, A., 2017. Interactions between temperature and drought in global and regional crop yield variability during 1961-2014. PLoS One 12, e0178339. https://doi.org/10.1371/journal.pone.0178339.
McKee, T.B., Doesken, N.J., Kleist, J., 1993. The relationship of drought frequency and duration to time scales. In: Proceedings of the 8th Conference on Applied Climatology. California, pp. 179–183.
Medellín-Azuara, J., Escriva-Bou, A., Rodríguez-Flores, J.M., Cole, S.A., Abatzoglou, J., Viers, J.H., Santos, N., Sumner, D.A., 2022. Economic Impacts of the 2020–22 Drought on California Agriculture.
Mohammed, S., Alsafadi, K., Enaruvbe, G.O., Bashir, B., Elbeltagi, A., Széles, A., Alsalman, A., Harsanyi, E., 2022. Assessing the impacts of agricultural drought (SPI/SPEI) on maize and wheat yields across Hungary. Sci. Rep. 12, 8838. https://doi.org/10.1038/s41598-022-12799-w.
Muñoz Sabater, J., 2019. ERA5-Land hourly data from 1950 to present. Copernicus Climate Change Service (C3S) Climate Data Store (CDS). https://doi.org/10.24381/cds.e2161bac last access: July 2025.
Naumann, G., Cammalleri, C., Mentaschi, L., Feyen, L., 2021. Increased economic drought impacts in Europe with anthropogenic warming. Nat. Clim. Change 11, 485–491. https://doi.org/10.1038/s41558-021-01044-3.
Naumann, G., Podesta, G., Marengo, J., Luterbacher, J., Bavera, D., Acosta Navarro, J., Arias-Muñoz, C., Barbosa, P., Cammalleri, C., Cuartas, L.A., 2023. Extreme and long-term Drought in the La Plata Basin: Event Evolution and Impact Assessment Until September 2022.
Osman, M., Zaitchik, B.F., Winstead, N.S., 2022. Cascading drought-heat dynamics during the 2021 Southwest United States Heatwave. Geophys. Res. Lett. 49. https://doi.org/10.1029/2022GL099265.
Pinke, Z., Decsi, B., Jámbor, A., Kardos, M.K., Kern, Z., Kozma, Z., Ács, T., 2022. Climate change and modernization drive structural realignments in European grain production. Sci. Rep. 12, 7374. https://doi.org/10.1038/s41598-022-10670-6.
Proctor, J., Zeppetello, L.V., Chan, D., Huybers, P., 2025. Climate change increases the interannual variance of summer crop yields globally through changes in temperature and water supply. Sci. Adv. 11. https://doi.org/10.1126/sciadv.ady3575.
Ray, D.K., Gerber, J.S., MacDonald, G.K., West, P.C., 2015. Climate variation explains a third of global crop yield variability. Nat. Commun. 6, 5989. https://doi.org/10.1038/ncomms6989.
Ribeiro, A.F.S., Russo, A., Gouveia, C.M., Páscoa, P., Zscheischler, J., 2020. Risk of crop failure due to compound dry and hot extremes estimated with nested copulas. Biogeosciences 17, 4815–4830. https://doi.org/10.5194/bg-17-4815-2020.
Running, S., Mu, Q., Zhao, M., 2015. MOD17A3H MODIS/terra Net Primary Production Yearly L4 Global 500m SIN Grid V006. NASA EOSDIS Land Processes Distributed Active Archive Center (DAAC) Data Set MOD17A3H-006.
Running, S.W., Nemani, R.R., Heinsch, F.A., Zhao, M., Reeves, M., Hashimoto, H., 2004. A continuous satellite-derived measure of global terrestrial primary production. Bioscience 54, 547–560.
Santini, M., Noce, S., Antonelli, M., Caporaso, L., 2022. Complex drought patterns robustly explain global yield loss for major crops. Sci. Rep. 12, 5792. https://doi.org/10.1038/s41598-022-09611-0.
SIAS – Servizio Informativo Agrometeorologico Siciliano, 2003. ANALISI METEO-CLIMATICA ANNO.
Team, R.C., 2016. R: a Language and Environment for Statistical Computing. R Foundation for Statistical Computing, Vienna, Austria. http://www.R-project.org/.
The MathWorks Inc, 2022. MATLAB Version: 9.13.0 (R2022B). The MathWorks Inc, Natick, Massachusetts.
Tripathy, K.P., Mishra, A.K., 2023. How unusual is the 2022 European compound drought and heatwave event? Geophys. Res. Lett. 50. https://doi.org/10.1029/2023GL105453.
Trnka, M., Rötter, R.P., Ruiz-Ramos, M., Kersebaum, K.C., Olesen, J.E., Žalud, Z., Semenov, M.A., 2014. Adverse weather conditions for European wheat production will become more frequent with climate change. Nat. Clim. Change 4, 637–643.
Verdugo, L., Bojórquez, A., Galaz, O., Romo-León, J.R., Sánchez-Mejía, Z.M., Yépez, E.A., Álvarez-Yépiz, J.C., 2024. Assessing two decades of landscape greenness in relation to temperature and precipitation in a tropical dry forest of Northwestern Mexico. Ecol. Indic. 166, 112369. https://doi.org/10.1016/j.ecolind.2024.112369.
Williams, A.P., Cook, B.I., Smerdon, J.E., 2022. Rapid intensification of the emerging southwestern North American megadrought in 2020–2021. Nat. Clim. Change 12, 232–234.
Williams, A.P., Cook, E.R., Smerdon, J.E., Cook, B.I., Abatzoglou, J.T., Bolles, K., Baek, S.H., Badger, A.M., Livneh, B., 2020. Large contribution from anthropogenic warming to an emerging North American megadrought. Science (1979) 368, 314–318. https://doi.org/10.1126/science.aaz9600.
Zhang, H., Loaiciga, H.A., Okujeni, A., Liu, J., Tan, M., Sauter, T., 2025. Assessing the impact of extreme climate events on European gross primary production. Agric. For. Meteorol. 362, 110374. https://doi.org/10.1016/j.agrformet.2024.110374.
Zhao, H., Zhang, L., Kirkham, M.B., Welch, S.M., Nielsen-Gammon, J.W., Bai, G., Luo, J., Andresen, D.A., Rice, C.W., Wan, N., Lollato, R.P., Zheng, D., Gowda, P.H., Lin, X., 2022. U.S. winter wheat yield loss attributed to compound hot-dry-windy events. Nat. Commun. 13, 7233. https://doi.org/10.1038/s41467-022-34947-6.
Zscheischler, J., Westra, S., van den Hurk, B.J.J.M., Seneviratne, S.I., Ward, P.J., Pitman, A., AghaKouchak, A., Bresch, D.N., Leonard, M., Wahl, T., Zhang, X., 2018. Future climate risk from compound events. Nat. Clim. Change 8, 469–477. https://doi.org/10.1038/s41558-018-0156-3.